

# Trapping of the Enoyl-Acyl Carrier Protein Reductase–Acyl Carrier Protein Interaction

Lorillee Tallorin,<sup>†</sup> Kara Finzel,<sup>†</sup> Quynh G. Nguyen, Joris Beld,<sup>‡</sup> James J. La Clair, and Michael D. Burkart\*

Department of Chemistry and Biochemistry, University of California, San Diego, 9500 Gilman Drive, La Jolla, California 92093-0358, United States

**S** Supporting Information

**ABSTRACT:** An ideal target for metabolic engineering, fatty acid biosynthesis remains poorly understood on a molecular level. These carrier protein-dependent pathways require fundamental protein–protein interactions to guide reactivity and processivity, and their control has become one of the major hurdles in successfully adapting these biological machines. Our laboratory has developed methods to prepare acyl carrier proteins (ACPs) loaded with substrate mimetics and cross-linkers to visualize and trap interactions with partner enzymes, and we continue to expand the tools for studying these pathways. We now describe application of the slow-onset, tight-binding inhibitor triclosan to explore the interactions between the type II fatty acid ACP from *Escherichia coli*, AcpP, and its corresponding enoyl-ACP reductase, FabI. We show that the AcpP–triclosan complex demonstrates nM binding, inhibits *in vitro* activity, and can be used to isolate FabI in complex proteomes.

Machines involved in primary metabolism, particularly the production of fatty acids, have garnered increased attention over the past decade due to their potential for biofuel production and as antibiotic targets. These machines share a common choreography, whereby acetyl-coenzyme A (CoA) and malonyl-CoA are assembled sequentially in an iterative fashion to form elongated fatty acids. All intermediates are tethered to an acyl carrier protein (ACP),<sup>1</sup> which carries its cargo along the assembly line of modifying partner enzymes until release by a thioesterase or transfer via an acyltransferase. While this modular machinery appears ideal for metabolic engineering, many of the leading efforts, such as heterologous pathway assembly,<sup>2</sup> have been met with limited success. We and others have shown that this arises from our lack of understanding the protein–protein interactions that guide the processivity between the ACP and its associated partner enzymes (Figure S1). Unfortunately, structural studies on these systems continue to pose challenges due to the transient nature of these interactions.

Our laboratory has developed a suite of tools to study the interactivity between ACP and associated enzymes through the chemoenzymatic preparation of ACPs that bear a diversity of tethered functionality on their pantetheine terminus.<sup>3</sup> These synthetic probes can be converted with CoaA, CoaD, and CoaE to the corresponding CoA analogs and *in situ* loaded onto the apo-ACP by the promiscuous 4'-phosphopantetheinyl trans-

ferase (PPTase) Sfp, resulting in a *crypto*-ACP bearing a terminal domain specific motif (Figure S2).<sup>4</sup> We now describe expansion of this approach to study enoyl reductase (ER) domains (Figure 1) using the enoyl-ACP reductase (FabI) from the *Escherichia coli* fatty acid synthase as a model. Understanding these protein–protein interactions is key to engineering and drug discovery efforts.

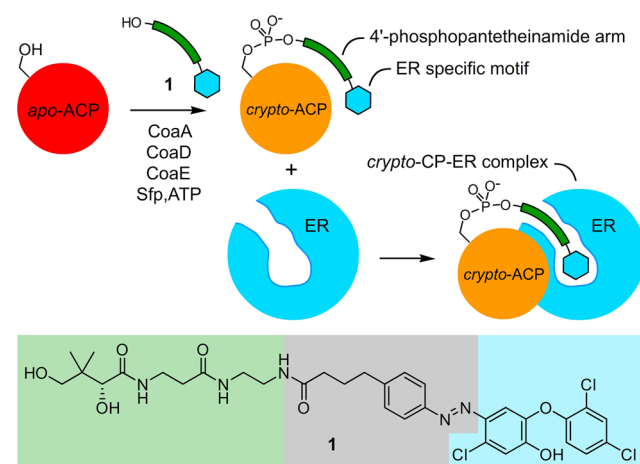


**Figure 1.** Developing ER probe 1 from triclosan (light blue), a linker (gray), and a pantetheine arm (green). An apo-ACP is chemoenzymatically modified with probe 1 yielding *crypto*-1-ACP, which contains the ER specific motif (blue hexagon). The resulting *crypto*-1-ACP can be used to bind to ER and trap the *crypto*-1-ACP–ER complex. A full depiction of the role of the ER in fatty acid biosynthesis is provided in Figure S1.

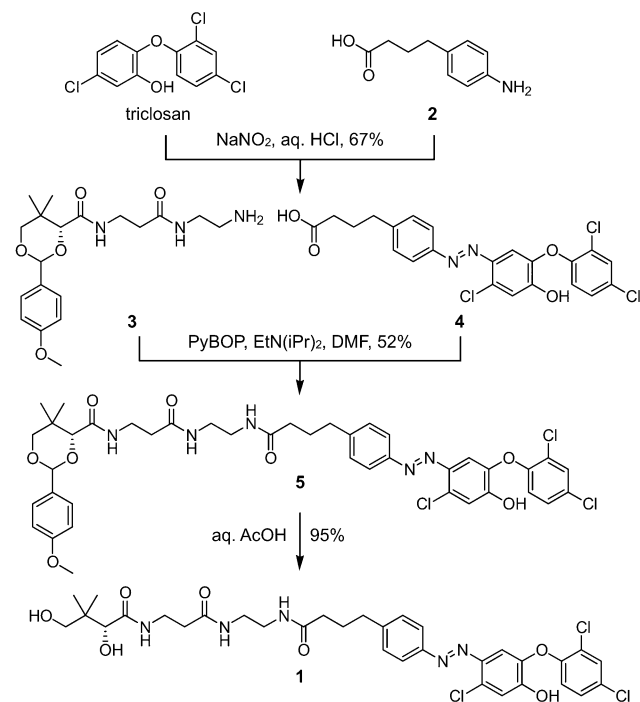
FabI, a member of the short chain alcohol dehydrogenase/reductase family, is responsible for the reduction of *trans*-2-enoyl-AcpP to acyl-AcpP via its NADH cofactor.<sup>5</sup> It is also characterized as playing a determinant role in completing cycles during fatty acid biosynthesis in *E. coli*.<sup>6</sup> As one of the eight ACP-partner protein structures, a 2.7 Å structure of the AcpP–FabI complex has been solved.<sup>7</sup> This structure contains a tetrameric FabI bound with two *trans*-2-dodecenoyl thioester loaded AcpPs. However, due to the transient nature of this interaction, the interface between AcpP and FabI was not well resolved.

**Received:** December 24, 2015

**Published:** March 3, 2016

We first sought to leverage our previous work with ketosynthase (KS), thioesterase (TE), and dehydratase (DH) domains (Figure S2)<sup>2,8</sup> and apply this approach to deliver ER domain probes. However, the design is complicated by the fact that ER enzymes typically do not involve covalent active site intermediates, but rather act via a NADH cofactor. We hypothesized that appending a tight noncovalent ER inhibitor<sup>9</sup> to the terminus of a pantetheinamide probe would, after chemoenzymatic loading, provide a *crypto*-ACP with sufficient binding to study ACP-ER interactions.<sup>10</sup> We began by exploring triclosan (Figure 1), a broad-spectrum antibiotic and prototypical inhibitor for FabI,<sup>11</sup> which is characterized by slow-onset, tight-binding inhibition. Previous studies have accounted this strong inhibition to the stable ternary complex formed when triclosan noncovalently interacts with both FabI and NAD<sup>+</sup>.<sup>12,13</sup> Additionally, it is suggested that AcpP interacts with basic residues adjacent to the FabI substrate binding loop. This loop is disordered in the FabI-cofactor binary complex and becomes ordered upon binding of NAD<sup>+</sup> and triclosan.<sup>7,14</sup>

### Scheme 1. Synthesis of the Triclosan Probe 1



We began by synthesizing probe 1 (Scheme 1), which is comprised of a pantetheine portion, a linker, and triclosan (Figure 1). The linker was developed from literature precedent,<sup>15</sup> based on it being long enough to span the distance between the AcpP and deep pocket of FabI. As depicted in Scheme 1, probe 1 was prepared in three steps from triclosan, 4-aminophenylbutyric acid (2), and amine 3. The synthesis began by forming a diazonium salt from 2 and NaNO<sub>2</sub> in the presence of HCl, which then was coupled *in situ* to triclosan via an electrophilic aromatic substitution. The resulting ~5:1 mixture of *trans*- to *cis*-azoacids 4<sup>15</sup> was coupled with 3 to yield 5 in 52% yield. Samples of probe 1 were achieved at 35% overall yield from triclosan after deprotection of 5 in aq. AcOH.

Our biochemical studies began by evaluating the inhibition of FabI. We found that 1 had an IC<sub>50</sub> value of 49.3 ± 0.2 μM

(Figure S3), which was 1000-fold greater (reduced affinity) than triclosan (IC<sub>50</sub> value of ~0.04 μM).<sup>13</sup> While this activity was less than desired, the slow off-rate associated with triclosan may still allow it to sufficiently trap ACP-ER complexes. Hence, we turned our attention to preparation of the corresponding *crypto*-1-AcpP.

Recombinant CoaA, CoaD, and CoaE were utilized to convert probe 1 into the corresponding CoA analog, which was used to post-translationally modify AcpP *in situ* using Sfp (Figure 1). We confirmed the loading of probe 1 onto apo-AcpP using conformationally sensitive urea-PAGE<sup>16</sup> (Figure S4) and LC-MS (ESI) analyses (Figure S5).

We used an affinity assay to explore the specificity of the *crypto*-1-AcpP to FabI (see schematic representation in Figure S6). FabI was covalently immobilized on Affi-Gel 10 resin and mixed with a panel of *crypto*-AcpPs to explore the selectivity of the domain specific motif. As seen in Figure 2a, only minimal

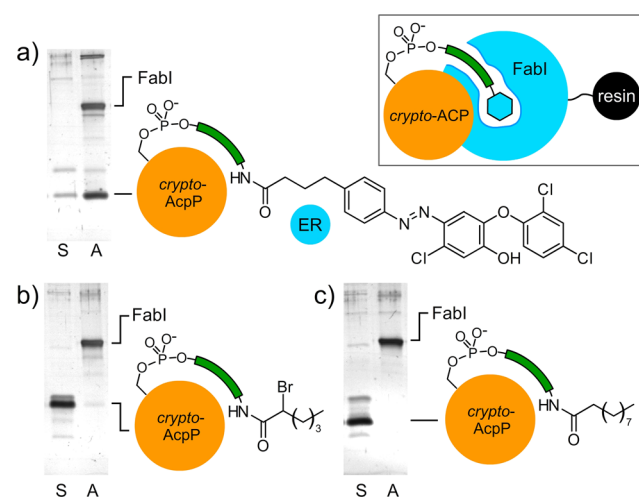


**Figure 2.** FabI resin was used to selectively isolate *crypto*-AcpP. SDS-PAGE gels shown from application of 20 μL of resin bearing 80 μM FabI to 20 μL of a solution containing 100 μM of (a) the ER specific *crypto*-1-AcpP. Negative controls including: (b) an α-bromoamide *crypto*-AcpP and (c) a fatty acid *crypto*-AcpP (see control probe structures in Figure S2). Lanes depict supernatant (S) from step 3 (Figure S6) and affinity (A) purified fractions from step 4 (Figure S6).

levels of *crypto*-1-AcpP were observed in the supernatant, while both FabI (released from the resin) and *crypto*-1-AcpP were largely observed in the affinity-isolated fraction, indicating that *crypto*-1-AcpP interacts with FabI. Alternatively, AcpP was not obtained when repeating the same procedure using two control probes bearing α-bromohexanoate (Figure 2b) and decanoate (Figure 2c) tethered to AcpP. This data indicated the binding of AcpP to FabI was only engaged when the ER domain-specific unit was present on the pantetheinamide terminus.

To further test selectivity for FabI, we reversed the affinity system. *Crypto*-1-AcpP was appended to Affi-Gel 10 and screened for its ability to isolate FabI from a series of lysates. As shown in Figure 3, *crypto*-1-AcpP resin was able to selectively isolate FabI from *E. coli* K12 lysate spiked with pure FabI (lysate 1, Figure 3), lysate from *E. coli* engineered to overexpress FabI (lysate 2, Figure 3), and *E. coli* K12 lysate (lysate 3, Figure 3).

Using purified recombinant proteins, we evaluated the ability of *crypto*-1-AcpP to inhibit FabI (Figure 4a). The inhibition of *crypto*-1-AcpP (IC<sub>50</sub> value of 1.1 ± 0.1 μM) (Figures 4a and S7)

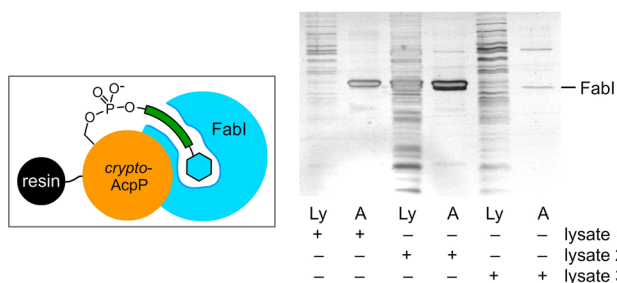


**Figure 3.** *Crypto-1-AcpP* resin was used to isolate FabI from different lysates (Ly). Lysate 1 contained 70  $\mu\text{L}$  of K12 lysate (1.0 mg/mL in total protein) spiked with 10  $\mu\text{L}$  of 80  $\mu\text{M}$  FabI. Lysate 2 contained 70  $\mu\text{L}$  of *E. coli* overexpressing FabI lysate (1.0 mg/mL in total protein). Lysate 3 contained 70  $\mu\text{L}$  of K12 lysate (1.0 mg/mL in total protein). Affinity isolated fractions (A) were generated by using 15  $\mu\text{L}$  of resin containing 75  $\mu\text{M}$  of the *crypto-1-AcpP*.

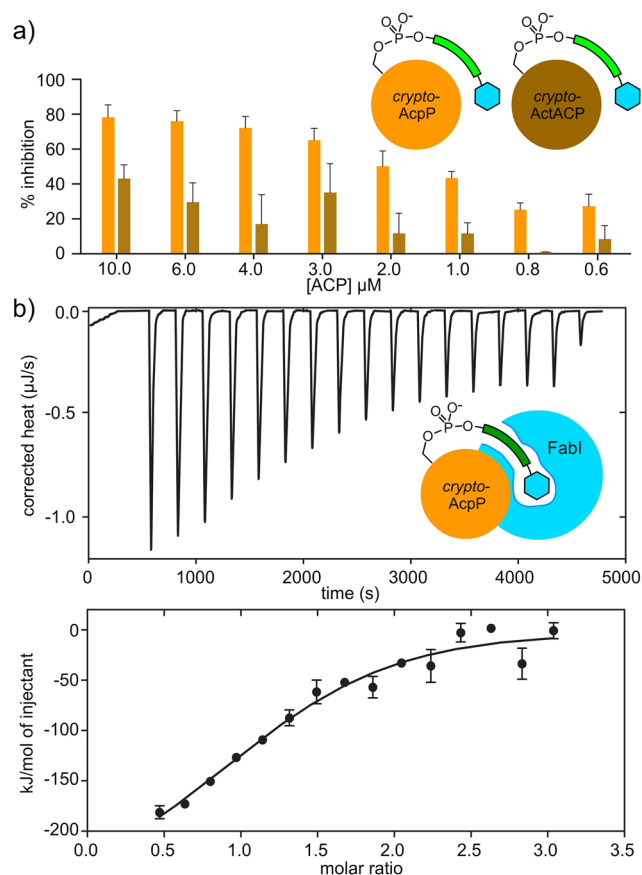


**Figure 4.** Inhibition and binding data. (a) Comparison of inhibition of 0.02  $\mu\text{M}$  FabI with either *crypto-1-ActACP* (brown) or *crypto-1-AcpP* (orange) at concentrations ranging from 0.15 to 10.0  $\mu\text{M}$ . (b) ITC analysis of the binding of *crypto-1-AcpP* to FabI. The initial concentration of the FabI monomer was 4.6  $\mu\text{M}$  in the cell and 18 injections of 3  $\mu\text{L}$  of 40  $\mu\text{M}$  *crypto-1-AcpP* were delivered sequentially. Data were collected in duplicate with a standard error <5%.

was 50-fold greater than probe 1 ( $\text{IC}_{50}$  value of  $49.3 \pm 0.2 \mu\text{M}$ ) (Figure S3), therein highlighting the importance of AcpP interactions.

Next, we tested the ability of FabI to discriminate cognate and noncognate carrier proteins. ActACP, the ACP from the type II actinorhodin polyketide synthase from *Streptomyces coelicolor*,<sup>17</sup> was loaded with 1 using the chemoenzymatic

labeling protocol (Figure 1). *Crypto-1-ActACP* did not show comparable inhibition of FabI to the cognate *crypto-1-AcpP* in the same range (Figure 4a). ActACP (PDB ID: 2K0X) docking studies with FabI structures (PDB IDs: 2FHS, 1DFI, and 1QSG) indicated no catalytically active orientation (Figure S8a). As opposed to AcpP, where 20% of structures show Ser36 pointing toward the FabI binding pocket (Figure S8b), the site of phosphopantetheine attachment on ActACP, Ser42, does not point toward the FabI active site (Figure S8a). No FabI inhibition was observed for *crypto-1-ActACP*, *crypto-acyl-AcpP*, *apo-AcpP*, or *holo-AcpP* (Figure S7) highlighting the importance of the loaded AcpP cargo.

Since probe 1 does not allow for covalent attachment of FabI and AcpP, we wondered whether the *crypto-1-AcpP* and FabI interaction was strong enough to stabilize the complex for future studies. We therefore utilized isothermal titration calorimetry (ITC) to measure the binding affinity of the two proteins (Figure 4b). Reports indicate that the 110.9 kDa FabI tetramer consists of monomers made up of seven  $\beta$ -strands packed by eight helices.<sup>7</sup> The resulting *crypto-1-AcpP* stoichiometry of binding was calculated to be 1:1 to each FabI monomer ( $n = 1.2 \pm 0.1$ ), suggesting that each site is independent and identical. Interestingly, the binding stoichiometry of *holo-AcpP* to the ketosynthase domain, KSII (FabF) from *E. coli*,<sup>18</sup> was also calculated to be 1:1. The FabI-AcpP crystal structure showed a stoichiometry of 2:1, albeit with poor resolution of the AcpP interface.<sup>7</sup>

We then explored the biophysical parameters guiding the interaction of *crypto-1-AcpP* to FabI. ITC analysis (Figure 4b) returned a  $K_d$  value of  $711.9 \pm 1.3 \text{ nM}$ , which is 3–10-fold lower than other AcpP-partner protein  $K_d$  values.<sup>19</sup> This interaction was exothermic, with  $\Delta G = -34.0 \pm 0.4 \text{ kJ/mol}$  ( $\Delta H = -234.9 \pm 26.7 \text{ kJ/mol}$ ) and had an entropic loss ( $\Delta S = -677.4 \pm 94.9 \text{ J}\cdot\text{mol}^{-1}\cdot\text{K}^{-1}$ ) characteristic of an enthalpy-driven binding event, presumably due to disorder of the protein–protein interaction.<sup>20</sup>

The present study extends our collection of chemoenzymatic AcpP tools with the first inhibitor-based noncovalent triclosan probe 1. This probe was appended to AcpP and was able to recognize and isolate FabI from complex lysates. The low micromolar inhibition of FabI with *crypto-1-AcpP* reveals a strong interaction of our proposed probe with FabI. This was further supported by the enhanced binding of *crypto-1-AcpP* to FabI.

Bacterial and apicomplexan ER domains from fatty acid synthases are currently targeted by several antibiotics, but resistance is increasing. Small molecules that disrupt the interface between AcpP and ER domains may offer a viable route for antibiotic design to combat resistance, but more structural information about this interaction is necessary. We envision the use of probe 1 or related probes to aid further structural characterization of the AcpP–ER interaction. A structural understanding of how ACPs interact with their cognate enzymes will also pave the way for metabolic engineering of biosynthetic pathways for the synthesis of pharmaceutically relevant metabolites, while also identifying essential ACP interactions in pathogenic organisms.

## ■ ASSOCIATED CONTENT

### Supporting Information

The Supporting Information is available free of charge on the ACS Publications website at DOI: 10.1021/jacs.5b13456.



Experimental details and data (PDF)

## AUTHOR INFORMATION

### Corresponding Author

\*[mburkart@ucsd.edu](mailto:mburkart@ucsd.edu)

### Present Address

<sup>‡</sup>Department of Microbiology and Immunology, Drexel University College of Medicine, 245 N 15th St, Philadelphia, PA 19107.

### Author Contributions

<sup>†</sup>These authors contributed equally.

### Notes

The authors declare no competing financial interest.

## ACKNOWLEDGMENTS

This work was supported by NIH R01 GM095970, NIH F31GM113470, and NSF IOS1516156. We would like to thank Drs. X. Huang and A. Mrse for NMR services (UC San Diego); Dr. Y. Su for MS services (UC San Diego); Dr. J. P. Noel (Salk Institute) and C. Vickery (UC San Diego) for assistance with Roche Lightcycler 480 and ITC studies; and Dr. C. Quinn (TA Instruments) for ITC experimental insight.

## REFERENCES

- (1) (a) Prescott, D. J.; Vagelos, P. R. *Adv. Enzymol. Relat. Areas Mol. Biol.* **2006**, *36*, 269. (b) Rock, C. O.; Cronan, J. E. *Biochim. Biophys. Acta, Lipids Lipid Metab.* **1996**, *1302*, 1.
- (2) Blatti, J. L.; Beld, J.; Behnke, C. A.; Mendez, M.; Mayfield, S. P.; Burkart, M. D. *PLoS One* **2012**, *7*, e42949.
- (3) Worthington, A. S.; Burkart, M. D. *Org. Biomol. Chem.* **2006**, *4*, 44.
- (4) (a) Nazi, I.; Koteva, K. P.; Wright, G. D. *Anal. Biochem.* **2004**, *324*, 100. (b) La Clair, J. J.; Foley, T. L.; Schegg, T. R.; Regan, C. M.; Burkart, M. D. *Chem. Biol.* **2004**, *11*, 195.
- (5) Bergler, H.; Fuchsbichler, S.; Högenauer, F.; Turnowsky, F. *Eur. J. Biochem.* **1996**, *242*, 689.
- (6) Heath, R. J.; Rock, C. O. *J. Biol. Chem.* **1995**, *270*, 26538.
- (7) Rafi, S.; Novichenok, P.; Kolappan, S.; Zhang, X.; Stratton, C. F.; Rawat, R.; Kisker, C.; Simmerling, C.; Tonge, P. J. *J. Biol. Chem.* **2006**, *281*, 39285. (b) Finzel, K.; Lee, D. J.; Burkart, M. D. *ChemBioChem* **2015**, *16*, 528.
- (8) Ishikawa, F.; Haushalter, R. W.; Lee, D. J.; Finzel, K.; Burkart, M. D. *J. Am. Chem. Soc.* **2013**, *135*, 8846.
- (9) (a) Pan, P.; Tonge, P. J. *Curr. Top. Med. Chem.* **2012**, *12*, 672. (b) Lu, H.; Tonge, P. J. *Acc. Chem. Res.* **2008**, *41*, 11.
- (10) (a) Saito, J.; Yamada, M.; Watanabe, T.; Iida, M.; Kitagawa, H.; Takahata, S.; Ozawa, T.; Takeuchi, Y.; Ohsawa, F. *Protein Sci.* **2008**, *17*, 691. (b) Rafi, S.; Novichenok, P.; Kolappan, S.; Zhang, X.; Stratton, C. F.; Rawat, R.; Kisker, C.; Simmerling, C.; Tonge, P. J. *J. Biol. Chem.* **2006**, *281*, 39285.
- (11) (a) Heath, R. J.; Yu, Y. T.; Shapiro, M. A.; Olson, E.; Rock, C. O. *J. Biol. Chem.* **1998**, *273*, 30316. (b) Swinney, D. C. *Nat. Rev. Drug Discovery* **2004**, *3*, 801. (c) Sivaraman, S.; Sullivan, T. J.; Johnson, F.; Novichenok, P.; Cui, G.; Simmerline, C.; Tonge, P. J. *J. Med. Chem.* **2004**, *47*, 509.
- (12) (a) Heath, R. J.; Rubin, J. R.; Holland, D. R.; Zhang, E.; Snow, M. E.; Rock, C. O. *J. Biol. Chem.* **1999**, *274*, 11110. (b) Qiu, X.; Abdel-Meguid, S. S.; Janson, C. A.; Court, R. L.; Smyth, M. G.; Payne, D. J. *Protein Sci.* **1999**, *8*, 2529. (c) Heath, R. J.; Su, N.; Murphy, C. K.; Rock, C. O. *J. Biol. Chem.* **2000**, *275*, 40128. (d) Kapoor, M.; Reddy, C. C.; Krishnasastri, M. V.; Surolia, N.; Surolia, A. *Biochem. J.* **2004**, *381*, 719.
- (13) (a) Ward, W. H.; Holdgate, G. A.; Roswell, S.; McLean, E. G.; Paupit, R. A.; Clayton, E.; Nichols, W. W.; Colls, J. G.; Minshull, C. A.; Jude, D. A.; Mistry, A.; Timms, D.; Camble, R.; Hales, N. J.;

Britton, C. J.; Taylor, I. W. *Biochemistry* **1999**, *38*, 12514. (b) Sivaraman, S.; Zwahlen, J.; Bell, A. F.; Hedstrom, L.; Tonge, P. *J. Biochemistry* **2003**, *42*, 4406. (c) Tallorin, L.; Durrant, J. D.; Nguyen, Q. G.; McCammon, J. A.; Burkart, M. D. *Bioorg. Med. Chem.* **2014**, *22*, 6053.

(14) (a) Nguyen, C.; Haushalter, R. W.; Lee, D. J.; Markwick, P. R.; Bruegger, J.; Caldara-Festin, G.; Finzel, K.; Jackson, D. R.; Ishikawa, F.; O'Dowd, B.; McGammon, A.; Opella, S. J.; Tsai, S. C.; Burkart, M. D. *Nature* **2013**, *505*, 427. (b) Zhang, Y. M.; Rao, M. S.; Heath, R. J.; Price, A. C.; Olson, A. J.; Rock, C. O.; White, S. W. *J. Biol. Chem.* **2001**, *276*, 8231. (c) Zhang, Y. M.; Wu, B.; Zheng, J.; Rock, C. O. *J. Biol. Chem.* **2003**, *278*, 52935.

(15) Brun, E. M.; Bonet, E.; Puchades, R.; Maquieira, A. *Environ. Sci. Technol.* **2008**, *42*, 1665.

(16) Rock, C. O.; Jackowski, S. *J. Biol. Chem.* **1982**, *257*, 10759.

(17) Haushalter, R. W.; Filipp, F. V.; Ko, K.; Yu, R.; Opella, S. J.; Burkart, M. D. *ACS Chem. Biol.* **2011**, *6*, 413.

(18) Worthington, A. S.; Porter, D. F.; Burkart, M. D. *Org. Biomol. Chem.* **2010**, *8*, 1769.

(19) (a) Arthur, C. J.; Williams, C.; et al. *ACS Chem. Biol.* **2009**, *4*, 625.

(20) Keskin, O.; Gursoy, A.; Ma, B.; Nussinov, R. *Chem. Rev.* **2008**, *108*, 1225–1244.